Smaller global and regional carbon emissions from gross land use change when considering sub-grid secondary land cohorts in a global dynamic vegetation model

Supplement Material

Chao Yue, Philippe Ciais, Wei Li

Laboratoire des Sciences du Climat et de l'Environnement, LSCE/IPSL, CEA-CNRS-UVSQ, Université Paris-Saclay, F-91191 Gif-sur-Yvette, France

Corresponding author: Chao Yue, chao.yue@lsce.ipsl.fr

Backcasting historical PFT maps and generation of land use change matrices

The processes to reconcile LUH1 land use transitions and the 2005 ORCHIDEE-compatible PFT map based on ESA CCI land cover map are summarized in Fig. S1. All land use transitions, as well as distribution of land use types or PFTs over model grid cells, are expressed as fraction of grid cell (unitless). The original land use transition matrices provided by LUH1 is M1. In Step S1, transitions from primary and secondary natural land are grouped together to derive the matrix M2, before they are split into forest and natural grassland. Next, land use transitions are separated into two types (Step S2) bearing the form of M3, which is further split into two matrices in Step S3: the net land use change matrix (M5), and the land turnover matrix (M4) that represents bi-directional equal-area transitions between two land cover types. Land turnover transitions are obtained by extracting the minimum value between two reverse land use transitions (secondary land and crop or pasture), with the rest (after subtracting this minimum) as the net transition. Here, the land turnover is limited to the tropical regions, as in the original LUH1 data.

In a circular process comprising the steps of S4 and S5, the net transition matrices for 1500-2004 are used with the 2005 PFT map as a starting point to iteratively backcast PFT map time series of 1500-2004 (Fig. S1). To make it simple, net transitions between pasture and cropland are ignored. Then natural lands are split into forest and natural grassland. This is described in Step S4, which generates the matrix M6. When splitting natural land into forest and grassland, increment in cropland or pasture is assumed as half being from forest, half from grassland; decrease in cropland is assumed to be occupied first by forest and then by grassland; decrease in pasture is assumed to be occupied half by forest and half by grassland. However, these rules must be consistent with the backcasting-dervied PFT map. For example, forest fraction in the previous year, which is going to be calculated as the sum of current-year forest lost (due to conversion to cropland) and its existing fraction, should simply not exceed unity (i.e., 100% of the grid cell area). In the opposite case, where forest fraction should be

calculated by subtracting a value from the current year fraction (because of cropland abandonment), the obtained value should not be lower than zero. These rules, despite simple ones at first glance, turn the backcasting historical PFT maps into a complex task with a lot compromises. In the worst case, compromises could not be made and part of the net transitions prescribed in the LUH1 data has to be ignored. This loop of generating PFT map for the former year using the current-year PFT map and the net transition matrix between the two years, finally generates annual time series of spatially resolved distribution of forest, natural grassland, cropland and pasture. The disaggregation of these four vegetation types further into model PFTs is done by assuming that their relative fractions conform to those for the year of 2005.

The next step is to make land turnover matrices being consistent with the backcasting-derived PFT map for each year. This is relatively easy to do. First, we restrict cropland-pasture land turnover rates within the minimum of existing fractions between cropland and pasture. Second, we restrict the turnover rates between secondary natural land and cropland (or pasture) within the minimum of existing fractions between secondary natural land and cropland (or pasture). Then the secondary natural land transitions are split into forest and grassland according to their current relative fractions. This process (Step S6) finally generates Matrix M7. The last task is to generate the matrices for wood harvest. Harvest information as grid cell fraction is provided for primary and secondary forest in LUH1 and maintained as the model input. However, the sum of their fractions is limited within existing forest area. Forest harvest matrices are represented as M8.

Fig. S2 – Fig. S6 explores the land use transition matrices over the globe after the backcasting constraint. Significant loss of information compared to the original LUH1 data happens for the case of net transition of natural land to pasture, where about 35% of natural land loss to pasture was suppressed (Fig. S2). This is an inevitable outcome given the irreconcilable discrepancy in the spatial distribution of land cover between the LUH1 and ESA CCI land cover map, as is detailed by Peng *et al.* (2017). However, areas for the four basic land use types, i.e., forest, grassland, cropland and pasture from our backcasting algorithm generally agree with those by Peng et al. (2017) (Fig. S3), who made the similar backcasting but used the cropland and pasture distribution map rather than land use transitions from LUH1 data, with forest area for 1850-2009 being constrained by data in Houghton (2003) based on national forest area statistics. Loss of land turnover information is less significant, with a historical maximum of ~30% for the transitions between secondary land and pasture (Fig. S4). Note that wood harvest by LUH1 data occurs for most forest biomes in the world, land turnover (literally shifting cultivation) is limited within tropical regions (Fig. S5). Finally, areas subject to wood harvest suffer almost no loss during the constraint in the backcasting process (Fig. S6).

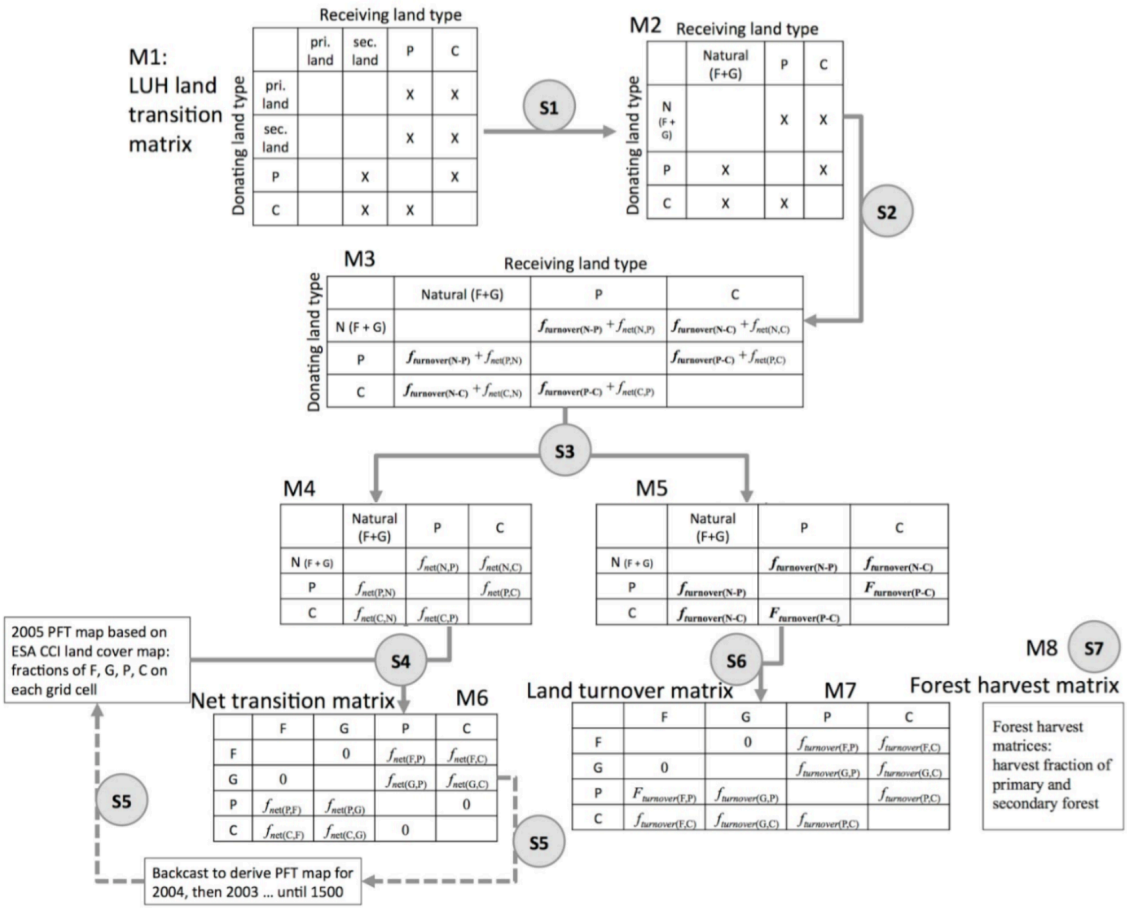

Fig. S1 Diagram illustrating the construction of time series of land transition matrices for net land use change, land turnover and wood harvest from LUH1 data set, and the backcasting of historical PFT map time series based on an ORCHIDEE-compatible PFT map, which is further derived from European Space Agency (ESA) Climate Change Initiative (CCI) land cover map covering the period of 2003-2008. M1 to M8 represent different matrices. M1 to M5 are intermediate matrices, M6 indicates the net transition matrix, M7 indicates the land turnover matrix, and M8 indicates forest harvest matrix. S1 to S5 represent different steps involved in deriving the M6-M8. S4 and S5 show a circular process of backcasting historical PFT map time series as constrained by net land use change matrices. Blank cells in the matrix indicate no transition occurring, while cells marked as '×' shows occurring transitions.

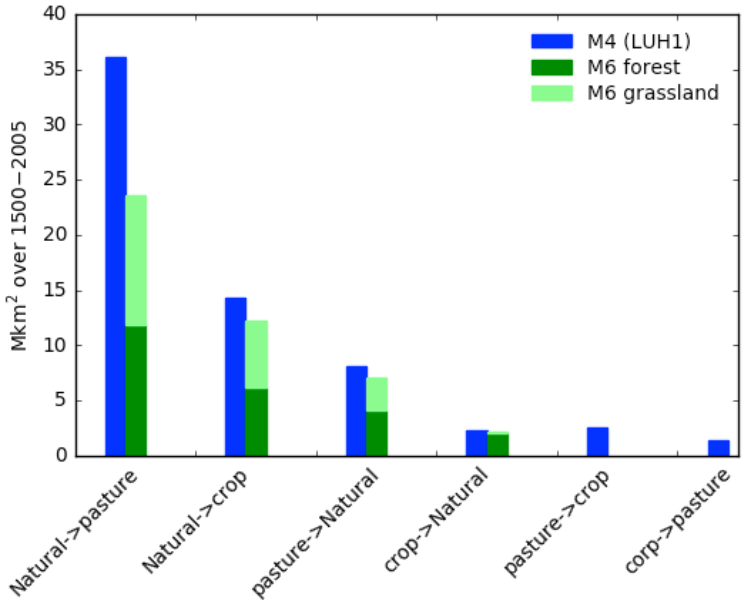

Fig. S2 The separation of natural land into forest (dark green) and natural grassland (light green) in the net land use transition matrices of M6, after the compromise with the 2005 PFT map, in comparison with the original values in LUH1 data set (M4). See Fig. S1 for details about matrices of M4 and M6.

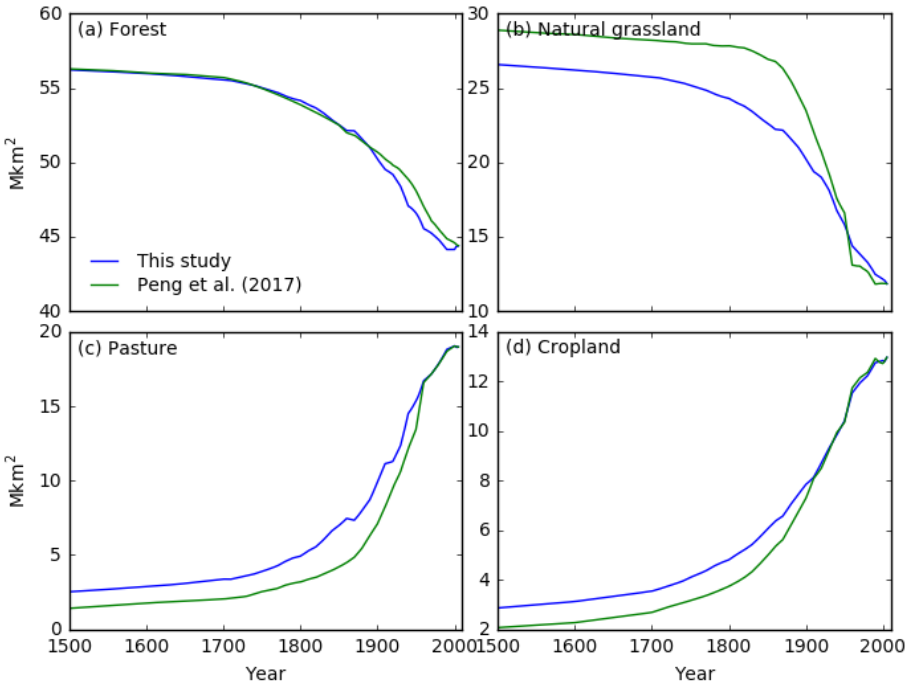

Fig. S3 The changes in areas of forest, natural grassland, pasture and cropland in comparison to Peng et al. (2017), who made the similar backcasting but used the cropland and pasture distribution map rather than land use transitions in LUH1 data, with forest area for 1850-2009 being constrained by data in Houghton (2003) based on national forest area statistics.

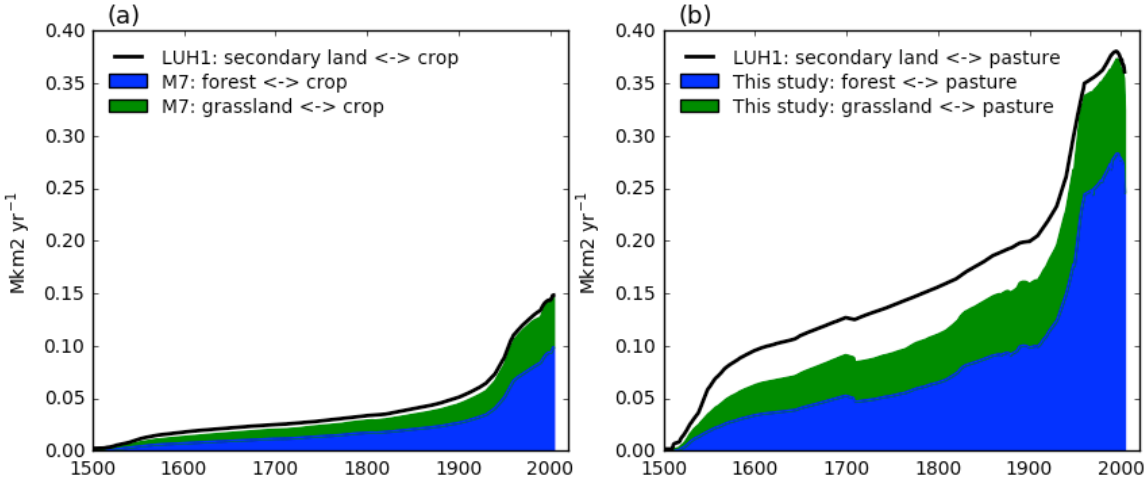

Fig. S4 Land turnover (i.e., shifting cultivation) originally contained in the LUH1 data indicated as reverse, equal-area land transitions between secondary natural land and, (a) cropland or (b) pasture, and with the land turnover transitions (between forest or natural grassland, and cropland or pasture) after constraint in our backcasting algorithm (M7).

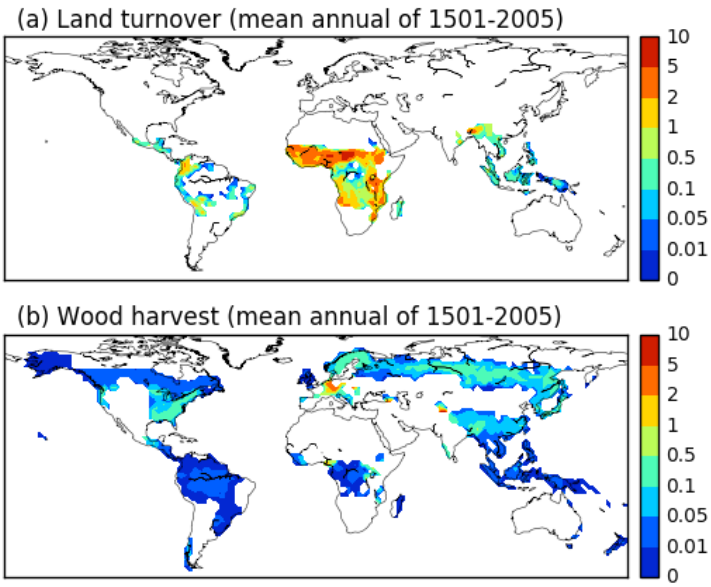

Fig. S5 Annual land turnover or forest harvest in percentage of grid cell area (%) averaged over 1501-2005.

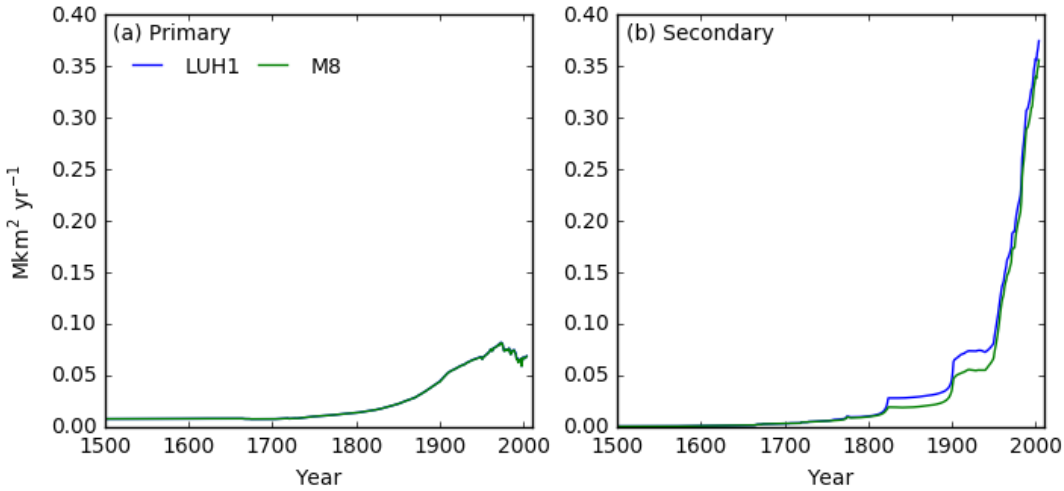

Fig. S6 Compare the time series of areas subject to wood harvest for (a) primary and (b) secondary forest, in the original LUH1 data and after the constraint in our backcasting algorithm (M8).

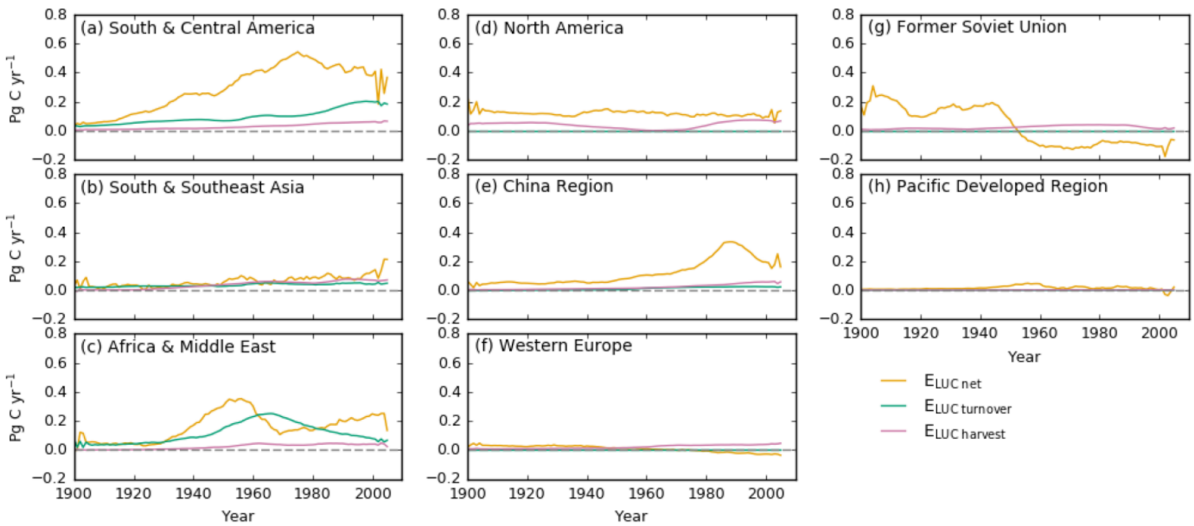

Fig. S7 Temporal pattern of regional land use change emissions (E_{LUC}) from different LUC processes for the $S_{ageless}$ simulation (i.e., without sub-grid age dynamics). The relative patterns of $E_{LUC\ net}$, $E_{LUC\ turnover}$ and $E_{LUC\ harvest}$ are similar in S_{age} simulation (with sub-grid age dynamics) and thus are not shown separately. Refer to Fig. 5 in the main text for the spatial extents of different regions.

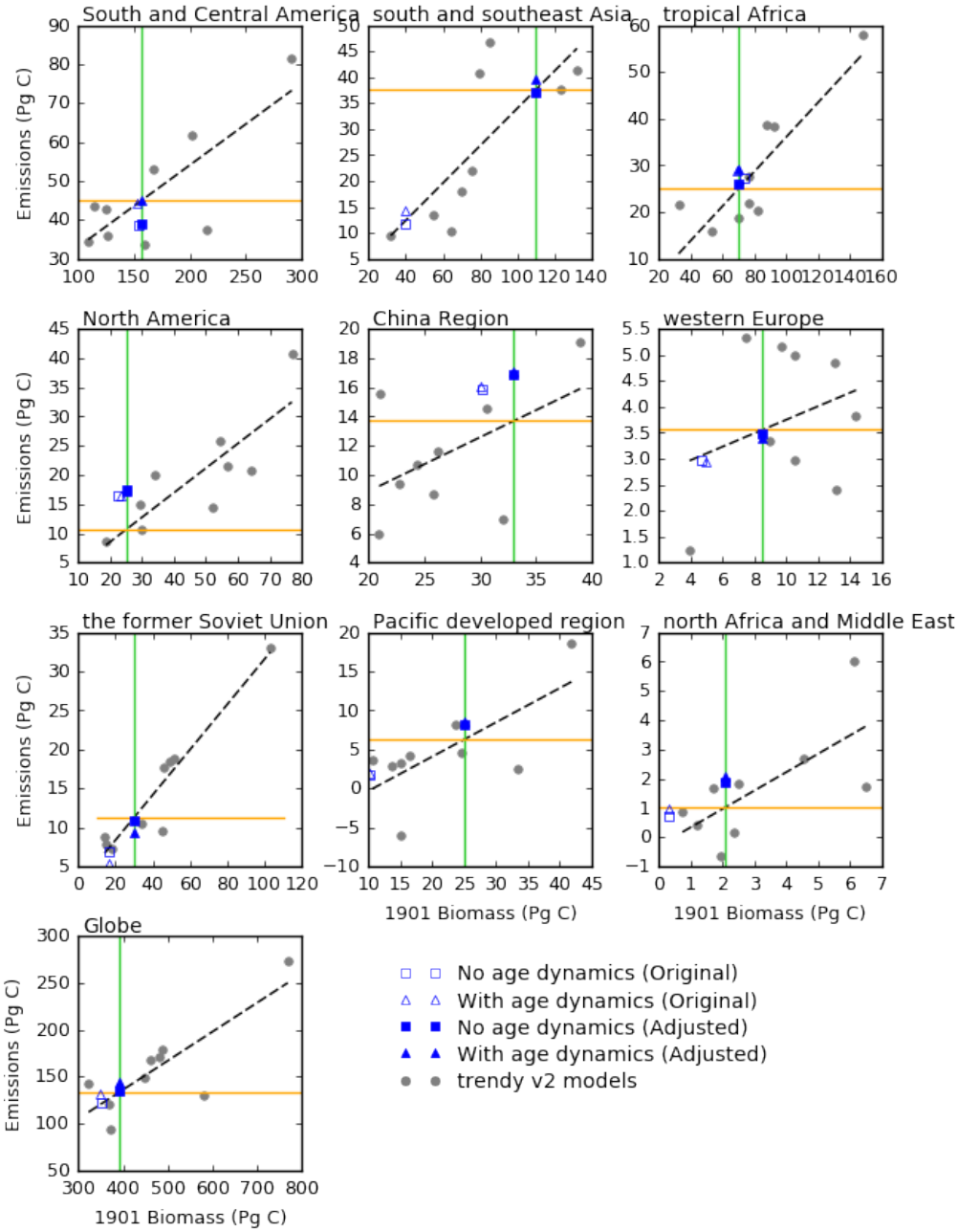

Fig. S8 Emergent relationship between estimated cumulative land use change emissions for 1901–2012 and initial total biomass carbon stock at 1901 among different dynamic global vegetation models of the Trends in Net Land-Atmosphere Exchange (TRENDY-v2) project, adapted from Li *et al.* (2017). Solid gray circles indicate TRENDY-v2 models, vertical green lines indicate observation-constrained reconstructed biomass stock at 1901, and horizontal orange lines indicate observation-constrained land use change emissions (E_{LUC}). Squares and triangles indicate simulated E_{LUC} by ORCHIDEE-MICT-GLUC without and with sub-grid secondary land cohorts, respective, with the empty squares/triangles for simulated E_{LUC} before biomass correction, and filled squares/triangles for simulated E_{LUC} after biomass correction.

Table S1 Comparisons of cumulative LUC emissions from our studies and several previous studies, adapted from Table 2 of Hansis *et al.* (2015).

Reference	Time period	LUC data set	LUC implementation[a]	Cumulative E_{LUC} (Pg C)
This study (With age dynamics, biomass adjusted)	*1850–2005*	*Hurtt et al. (2011)*	*GT, WH*	*161-194*
This study (With age dynamics, original)	*1850–2005*	*Hurtt et al. (2011)*	*GT, WH*	*147*
This study (No age dynamics, biomass adjusted)	*1850–2005*	*Hurtt et al. (2011)*	*GT, WH*	*174-207*
This study (No age dynamics, original)	*1850–2005*	*Hurtt et al. (2011)*	*GT, WH*	*158*
Hansis et al. 2015	1850–2005	Hurtt et al. (2011)	GT, WH, AProp	261
Houghton et al. (2012) multimodel range	1920–1999	various	various	72–115
Houghton (personal communication)	1850–2010	FAO/FRA (on regional basis)	GT, WH, APasture	182
Shevliakova et al. (2013)	1850–2005	Hurtt et al. (2011)	GT, WH, AProp	210
Jain et al. (2013)	1900–2005	various	NT, WH, AProp	160–178
Stocker et al. (2014)	1850–2004	Hurtt et al. (2011)	GT, WH, AProp	171
Wilkenskjeld et al. (2014)	1850–2005	Hurtt et al. (2011)	GT, WH, APasture	225
Gasser and Ciais (2013), Hurtt	1850–2005	Hurtt et al. (2011) (on regional basis)	GT, WH, AProp	294
Gasser and Ciais (2013), Hurtt/Houghton	1850–2005	Hurtt et al. (2011) (on regional basis)	GT, WH, AProp	203

[a]Implementation choices refer to gross (subgrid-scale) versus net LUC transitions (GT versus NT), if wood harvest is included (WH) and if agricultural land is taken proportionally from natural vegetation types (AProp) or if pasture is preferentially taken from grasslands (APasture). In our study, agricultural land is taken equally from forest and natural grassland, then proportionally within all forest or grassland PFTs.

Table S2 Original and biomass-corrected cumulative E_{LUC} estimates for 1501–2005, 1850–2005 and 1901–2005 using the emergent relationship between cumulative E_{LUC} and initial biomass in 1901, and observation-based reconstructed biomass in 1901 from Li et al. (2017), See also Fig. S8.

	No age dynamics				With age dynamics			
	1501–	**1850–**	**1901–**	**1901– Ratio**	**1501–**	**1850–**	**1901–**	**1901– Ratio**
Original estimates								
South and Central America	49.8	47.3	44.4		41.0	40.2	38.5	
south and southeast Asia	17.7	15.7	14.2		14.1	13.0	11.7	
tropical Africa	44.2	31.9	28.8		34.7	29.3	27.3	
North America	27.5	25.2	16.5		28.2	25.7	16.4	
China Region	27.3	17.6	16.0		26.7	17.3	15.9	
western Europe	9.2	4.6	2.9		9.7	4.7	3.0	
the former Soviet Union	19.1	12.2	5.4		21.0	13.9	6.9	
Pacific developed region	2.6	2.2	2.0		2.5	2.0	1.7	
north Africa and Middle East	1.2	1.1	1.0		1.0	0.9	0.7	
Globe	198.7	157.7	131.3		178.8	146.9	122.1	
Biomass-corrected estimates								
South and Central America	50.7	48.2	45.2	1.02	41.6	40.8	39.1	1.02
south and southeast Asia	49.3	43.9	39.7	2.79	44.4	40.9	37.0	3.15
tropical Africa	44.7	32.2	29.1	1.01	32.9	27.8	25.9	0.95
North America	28.7	26.2	17.2	1.04	30.2	27.5	17.5	1.07
China Region	29.1	18.8	17.1	1.07	28.5	18.5	16.9	1.07
western Europe	10.7	5.3	3.4	1.16	11.3	5.5	3.5	1.17
the former Soviet Union	32.7	20.8	9.3	1.71	32.9	21.8	10.9	1.57
Pacific developed region	11.5	9.6	8.5	4.33	12.0	9.6	8.3	4.85
north Africa and Middle East	2.6	2.3	2.1	2.15	2.4	2.1	1.9	2.51
Globe	218.9	173.7	144.6	1.10	196.1	161.1	134.0	1.10
Globe (as sum of regions)	260.0	207.3	171.6	-	236.1	194.5	160.9	-

References:

Hansis E, Davis SJ, Pongratz J (2015) Relevance of methodological choices for accounting of land use change carbon fluxes. *Global Biogeochemical Cycles*, **29**, 2014GB004997.

Houghton RA (2003) Revised estimates of the annual net flux of carbon to the atmosphere from changes in land use and land management 1850–2000. *Tellus B*, **55**, 378–390.

Li W, Ciais P, Peng S et al. (2017) Land-use and land-cover change carbon emissions between 1901 and 2012 constrained by biomass observations. *Biogeosciences Discuss.*, **2017**, 1–25.

Peng S, Ciais P, Maignan F, Li W, Chang J, Wang T, Yue C (2017) Sensitivity of land use change emission estimates to historical land use and land cover mapping. *Global Biogeochemical Cycles*, **31**, 2015GB005360.